SPACE-WEATHERING SPECTRA EXPLAINED WITH LIGHT SCATTERING SIMULATIONS. A. Penttilä[1], T. Väisänen[1], J. Markkanen[1,2], J. Martikainen[1], J. Escobar-Cerezo[1], T. Kohout[4], G. Videen[3], and K. Muinonen[1,5], [1]Department of Physics, P.O. box 64, 00014 University of Helsinki, Finland (antti.i.penttila@helsinki.fi), [2]Max Planck Institute for Solar System Research, Göttingen, Germany, [3]Space Science Institute, Boulder, Colorado, USA, [4]Department of Geosciences and Geography, University of Helsinki, Finland, [5]Geospatial Research Institute FGI, National Land Survey, Kirkkonummi, Finland.

Introduction: Space weathering (SW) of regolith particles on the surfaces of atmosphereless Solar System bodies is a mechanism that has been actively studied since the Apollo lunar samples (see, e.g., [1] and references therein). The mechanism has been verified in laboratory experiments and recently by studying samples from asteroid (25143) Itokawa by the Hayabusa mission [2]. It has been identified that the spectral features associated with SW, namely the darkening and reddening of the spectra, are caused by nano- and microphase Fe inclusions in the thin rim of the regolith particles (see, e.g., [3]).

Until now, the physical first-principles model of the SW effects on spectra by Fe inclusions has been lacking. Extensive work has been done in this field using the Hapke model(s) (e.g., [4–6]), but the model is an approximation of a radiative transfer treatment. One deficiency in the model is the lack of a proper treatment of the size effects of the Fe inclusions. Lucey and Riner[7] assessed this by including Mie scattering for the inclusions. However, current state-of-the-art modeling is missing a proper treatment of (*i*) surface reflections and volume scattering, and (*ii*) multiple scattering and incoherent fields associated with the inclusions.

We have recently completed a project aimed at improving the theory and computational tools for radiative transfer–type solutions in dense particulate media [8–10]. These are combined with our existing tools for light-scattering simulations with surface and volume scattering [11,12]. Using these light-scattering simulation tools, we develop a detailed view on how the Fe inclusions affect the spectra of non-weathered silicate minerals.

Spectral modeling. The nano- and micro-Fe inclusions have been seen to (*1*) decrease the overall reflectance of the regolith, (*2*) decrease the absorption band depths, and (*3*) introduce a red slope. Example spectra of fresh olivine and laboratory-produced SW analog samples are shown in Fig. 1.
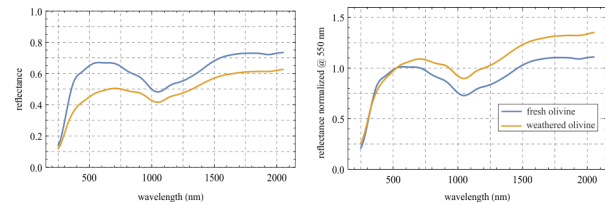

Figure 1. Measured spectra of fresh and weathered olivine on absolute reflectance scale (left) and normalized at the 550-nm wavelength (right). For details about the sample preparation, see [13].

The scattering simulations require knowledge of the complex refractive indices *m* of the materials. For iron we employ the most recent work by Cahill et al. [14]. For olivine, we use the data for Stubachtal olivine from the Jena Database of Optical Constants for Cosmic Dust. The real and imaginary parts (i.e., scattering and absorption coefficients) of *m* are shown in Fig. 2.
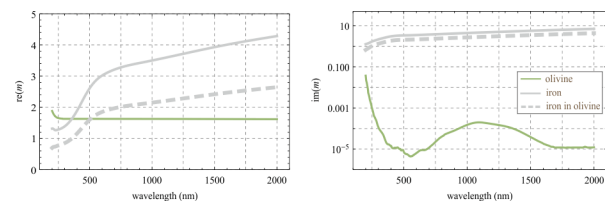

Figure 2. The real (left) and imaginary (right) parts of the refractive index for olivine and iron in vacuum, as well as for iron in olivine.

Mechanisms for different spectral effects. Before entering full-range simulations of the SW spectral effects, we try to understand the different mechanisms behind the effects on a conceptual level. First, (*1*) the overall decrease of reflectance is straightforward. In SW, iron is separated from the mineral matrix and forms inclusions close to and over the size of the wavelength. The imaginary part of m_{Fe} governing the absorption is large, so the overall albedo is reduced.

Second, (*2*) the decrease of the absorption bands is also straightforward using the non-linear Beer-Lambert behavior of the absorption and effective-medium models. The brighter parts of the spectra for fresh olivine are due to the material having very small absorption coefficient *k*, while for the absorption bands the coefficient *k* is already larger. Adding a small amount of nanophase Fe, according to effective-medium models, adds more-

or-less constant amount to the effective k. Now assuming Beer-Lambert $\exp(-kl)$ absorption over a distance l, a constant increase to a small initial k has a large darkening effect, while the same constant increase to an initially larger k has a smaller effect. That is why the bright parts of the spectra will darken more than the absorption bands in SW, smoothening the spectra.

Finally, (*3*) the red slope is a consequence of the size effects of the Fe inclusions. In Fig. 3, we show how the absorption efficiency Q_{abs} behaves for three different-sized spherical Fe inclusions as a function of the wavelength. The small inclusions (i.e., nanophase Fe) are especially efficient in absorption when the wavelength is close to their size, but the efficiency decreases fast with larger wavelengths. This will decrease the brightness in small wavelength, while not so much for larger wavelengths, resulting in a red slope in the spectrum.
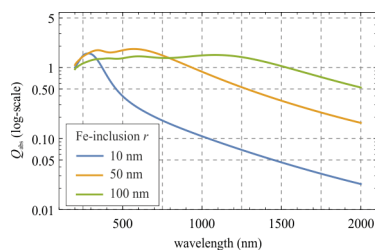

Figure 3. Absorption efficiency as a function of wavelength for three sizes of Fe spheres in olivine.

Full-scale light-scattering simulations for the SW effects. To properly validate the conceptual explanations we introduced above, we will run extensive simulations on the spectral behavior of fresh and weathered olivine. We will employ our recent models with a multiple-scattering incoherent-field treatment for the Fe inclusions in the olivine matrix, using the FaSTMM code [15]. The resulting scattering properties of an average volume element of olivine with Fe inclusions is then inserted into the surface layer of the regolith grain model using the recent version of the SIRIS code, capable of modeling core-mantle Gaussian random particles. Finally, a multiple scattering simulation between many grains forming a layer of regolith is simulated. A somewhat similar simulation pipeline is described in [12].

Discussion. On a conceptual level, we have a good understanding of the light-scattering mechanisms that cause the observed spectral effects in space-weathered minerals. We will validate these hypotheses with light-scattering simulations that are designed for radiative transfer in particulate media.

As the simulations can reproduce the observed SW effects, they can be trusted to be used in predicting spec-

tral effects with, e.g., varying amounts of Fe, other inclusion material than Fe, and effects in the UV wavelengths.

UV bluing. Regarding the SW spectral effect in UV, especially the so-called UV bluing (see, e.g., [6,16], we can clarify some open questions. For example, at least with the refractive indices used in this work (Fig. 2) starting from the wavelength of 200 nm, we see no evidence of *absolute spectral bluing* with SW. The absorption coefficient of olivine increases rapidly in UV, resulting in a rapid decrease in reflectance. However, the Fe absorption coefficient is still larger, so the fresh olivine reflectance continues to be larger than that of the SW olivine *in the absolute scale*. However, the difference between fresh and SW olivine is largest close to a wavelength of 550 nm. If the reflectance is normalized at that wavelength, the *relative reflectance* of fresh olivine in UV can even supersede the SW olivine. While this might give the impression of UV bluing when comparing the fresh and weathered material, the effect is not real in the absolute scale. Furthermore, the reflectance of both fresh and weathered minerals is very low in UV, making this wavelength range difficult for observations. The space-weathering effects are seen much more prominently close to 550 nm, where fresh olivine has a local minimum in the absorption coefficient.

References: [1] Hapke B. (2001) *J Geophys Res 106*, 10039–10073. [2] Matsumoto et al. (2015) *Icarus 257*, 230–238. [3] Pieters C.M. and Noble S.K. (2016) *J Geophys Res Planets 121*, 1865–1884. [4] Lawrence S.J. and Lucey P.G. (2007) *J Geophys Res 112*, E07005. [5] Nimura T. et al. (2008) *Earth Planets Space 60*, 271–275. [6] Vilas F. and Hendrix A.R. (2015) *Astron J 150(2)*. [7] Lucey P.G. and Riner M.A. (2011) *Icarus 212*, 451–462. [8] Muinonen K. et al. (2018) *Opt Lett 43(4)*, 683–686. [9] Markkanen J. et al. (2018) *Opt Lett 43(12)*, 2925–2928. [10] Väisänen T. et al. (2019) *PLOS One*, in press. [11] Muinonen K. et al. (2009) *J Quant Spectrosc Radiat Transf 110*, 1628–1639. [12] Martikainen J. et al. (2018) *Mon Not R Astron Soc 483(2)*, 1952–1956. [13] Kohout et al. (2014) *Icarus 237(15)*, 75–83. [14] Cahill J.T.S et al. (2019) *Icarus 317*, 229–241. [15] Markkanen J. and Yuffa A.J. (2017) *J Quant Spectrosc Radiat Transf 189*, 181–188. [16] Brown A.J. (2014) *Icarus 239*, 85–95.